Journal of Materials Chemistry A

β-Functionalized Push-Pull Opp-Dibenzoporphyrins as Sensitizers for Dye-Sensitized Solar Cells: The Push Group Effect

Journal:	*Journal of Materials Chemistry A*
Manuscript ID	TA-ART-09-2021-007814.R1
Article Type:	Paper
Date Submitted by the Author:	08-Nov-2021
Complete List of Authors:	Hu, Yi; University of North Texas, Chemistry Alsaleh, Ajyal; University of North Texas, Chemistry Trinh, Oanh Thi Phuong; University of North Texas, Chemistry D'Souza, Francis; University of North Texas, Chemistry Wang, Hong; University of North Texas, Chemistry

SCHOLARONE™
Manuscripts

Journal Name

ARTICLE

β-Functionalized Push-Pull *Opp*-Dibenzoporphyrins as Sensitizers for Dye-Sensitized Solar Cells: The Push Group Effect

Received 00th January 20xx,
Accepted 00th January 20xx

DOI: 10.1039/x0xx00000x

www.rsc.org/

Yi Hu,[a,‡] Ajyal Alsaleh,[a,‡] Oanh Trinh,[a] Francis D'Souza*[a] and Hong Wang*[a]

β-Functionalized push-pull zinc *opp*-dibenzoporphyrins were designed and synthesized as sensitizers for dye-sensitized solar cells. The utilization of arylamine to replace aliphatic amine as the donor groups has been proved to be an effective strategy to solve the solar cell instability reported previously. Three different arylamino groups including carbazole (**YH8**), diphenylamine (**YH9**), and phenothiazine (**YH10**) were investigated as the arylamine donor groups, and different electronic effects were observed for these donor groups. Diphenylamine carrying **YH9** and phenothiazine carrying **YH10** displayed strong push-pull characteristics including segregated HOMO/LUMO and red-shifted and broadened absorption bands. In sharp contrast, the incorporation of carbazole (**YH8**) cancels out the push-pull effect. **YH9** and **YH10** solar cells achieved high PCE of 6.9% and 7.5% respectively, which are comparable to that of the best ruthenium dye, **N719** (η = 7.7%), under similar conditions. This work demonstrates the great potentials of π-extended porphyrins as sensitizers for dye-sensitized solar cells.

1. Introduction

Dye-Sensitized Solar Cells (DSSC) offer a cheap and convenient solution for clean and renewable energy. Due to the critical role dyes plays in DSSC, extensive efforts have been devoted to developing suitable dyes for DSSC.[1-9] Porphyrin is one of the most investigated dyes in the past decade.[7, 10-12] Porphyrins possess a number of properties that are suitable for DSSCs including broad absorptions in the visible region and favorable cell kinetics for electron injection and charge recombination. The push-pull porphyrins introduced by Diau and Yeh represent an extremely successful development of organic dyes.[13] Record-breaking power conversion efficiencies (PCEs) for DSSC have been achieved with these push-pull porphyrins.[13-25] Despite these advances, DSSCs based on organic dyes are still far from practical applications due to problems relating to solar cell instability arising from labile anchoring group,[26-28] lengthy synthesis, and low photostability of dyes. The development of DSSCs has reached a bottleneck. New strategies must be developed in order to make new breakthroughs in DSSC.

π-Extended porphyrins are attractive candidates as sensitizers for DSSC. As compared to their parent porphyrins, π-extended porphyrins display broader and red-shifted absorptions with often enhanced Q bands, which allow more effective overlap with the solar spectrum.[29-40] However, due to difficult synthesis and lack of functionalization methods, despite of their interesting optical and photophysical properties, π-extended porphyrins have been rarely used in DSSC and other

Our previous work: β-functionalized push-pull dibenzoporphyrins carrying phenylethynyl bridge

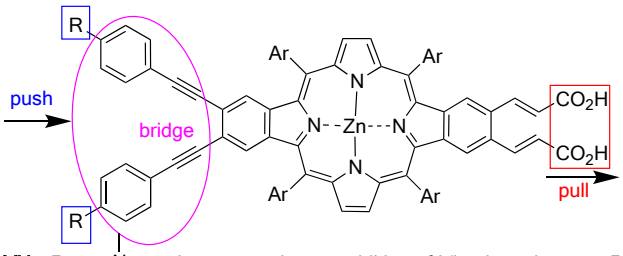

YH7, R = , decomposed upon addition of I^-/I_3^- electrolyte, η = 5.7 %

YH6, R = H, stable upon addition of I^-/I_3^- electrolyte, η = 6.7 %

This work: push group effect on β-functionalized push-pull dibenzoporphyrins

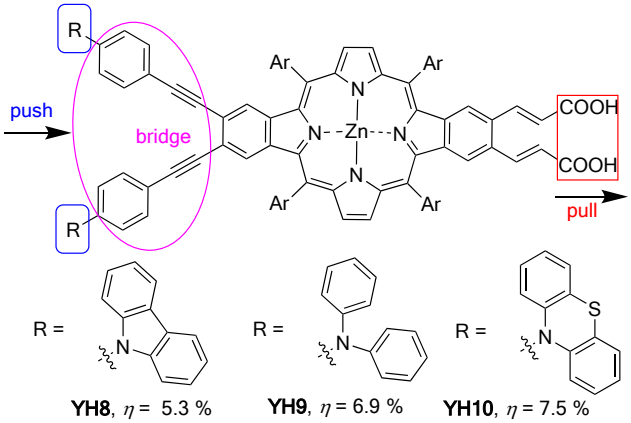

YH8, η = 5.3 % **YH9**, η = 6.9 % **YH10**, η = 7.5 %

Figure 1 β-Functionalized push-pull π-extended porphyrins

[a] *Department of Chemistry, University of North Texas, 1155 Union Circle, #305070, Denton, TX 76203-5017, USA*
[b] ‡ *equal contribution*
Email: hong.wang@unt.edu; francis.dsouza@unt.edu
Electronic Supplementary Information (ESI) available: See DOI: 10.1039/x0xx00000x

Please do not adjust margins

applications.[41-51] Our groups have been engaged in developing concise and versatile synthetic methods to access linearly π-extended porphyrins.[52-55] The availability of these methods has opened the door to design functionalized π-extended porphyrins. Through developing new classes of push-pull π-extended porphyrins as sensitizers for DSSC, we wish to provide new opportunities in the field of dye-sensitized solar cells.

In a previous work, we designed a class of push-pull dibenzoporphyrin (**YH7**), which bear dimethylamino groups on phenylethynyl bridge as the "push" (electron-donating) group and acrylic acid as the "pull" (electron-withdrawing or anchoring) group (Fig. 1, top).[56] **YH7** displayed strong "push-pull" effect including much faster electron-ejection from the excited state to the conduction band of TiO_2, pronounced HOMO and LUMO orbital segregation, and broadened and enhanced absorption bands, all of which suggest that better power conversion efficiency (PCE) should be obtained for the **YH7**-based solar cell. To our surprise, **YH7** showed lower PCE than its non-push-pull analogue **YH6**. Careful investigation has revealed that **YH7** has similar or increased stability with its non-push-pull analogue **YH6** in solution and on TiO_2 surface. However, significant illumination-induced photodegradation of **YH7** was observed when electrolyte I^-/I_3^- was present. In order to solve the decomposition problem, we have designed a new series of push-pull dibenzoporphyrins bearing tertiary arylamine groups as the electron-donating group (Fig. 1, bottom). Our studies have shown that the decomposition problem has been resolved through incorporating tertiary arylamines and much enhanced PCE similar to that of the best Ruthenium dye (**N719**) has achieved. Herein, we present the synthesis, studies on donor group effect and structure-property relationships of these push-pull *opp*-dibenzoporphyrins, and their evaluation as sensitizers in DSSCs.

2. Results and discussion

2.1 Molecular design and synthesis

The low photostability of push-pull dibenzoporphyrin **YH7** in the presence of I^-/I_3^- electrolyte likely arose from the redox reaction between the excited dye with the I^-/I_3^- electrolyte. Although triethanolamine (TEA) has been reported to facilitate photobleaching of porphyrins,[57] such photodegradation has not been reported for other dyes carrying amino groups. Considering **YH6** which does not carry amino groups and does not decompose in the presence of I^-/I_3^- electrolyte, the dimethylamino groups on **YH7** appeared to be responsible for the severe photodegradation. In order to solve this problem, we decided to replace the dimethylamino group on **YH7** with diarylamino groups. Diarylamino derivatives are electron-rich compounds that have been used as hole transporting materials and light emitter in the field of optoelectronics.[58] Diarylamine has been reported to promote fast regeneration reaction in DSSC through repelling the triiodide ions from the TiO_2 surface to reduce charge recombination.[59] Very importantly, diarylamine is expected to be more stable in its excited state due to the delocalization of the excited radical into the π-

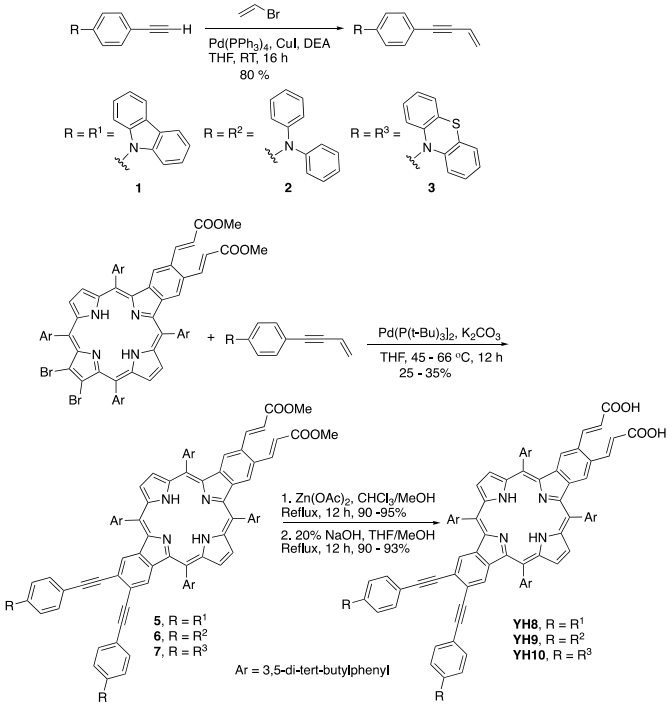

Scheme 1 Synthesis of starting enynes and push-pull dibenzoporphyrins bearing 3° arylamine groups

system. We have designed a homologous set of push-pull zinc dibenzoporphyrins bearing tertiary arylamines including carbazole (**YH8**, Fig. 1), diphenylamine (**YH9**) and phenothiazine (**YH10**) as the donor group, and acrylic acid groups as the pull/anchoring groups. Triphenylamine derivatives have been extensively studied as electron-donating units in various porphyrin dyes.[27] Carbazole and phenothiazine are structurally analogous to the triphenylamine unit except that the two phenyl rings are fused together through a 5-membered ring (carbazole) and 6-membered ring (phenothiazine), respectively. The fusion would force two phenyl groups to lie in the same plane, further extending the π-conjugation. The presence of the sulfur atom in phenothiazine (**YH10**) is also expected to have impacts on its electronic structures.

The synthesis of these push-pull dibenzoporphyrins is illustrated in Scheme 1. The three donor diarylamine derivatives **1, 2** and **3** were synthesized from ethynylbenzenes, which were either commercially available or prepared using literature reported procedures,[60] via Sonogashira coupling reaction. Dibromobenzoporphyrin **4** was synthesized using a similar procedure reported previously by us.[54, 61, 62] Dibromobenzoporphyrin **4** reacted with the corresponding enynes through the Heck-based sequence reaction, which involves the Heck reaction followed by 6π-cyclization and subsequent aromatization, yielded *opp*-dibenzoporphyrins **5**, **6** and **7**. The Heck reactions were carried out in the presence of $Pd[P(t\text{-}Bu)_3]_2$. No oxidant was needed for 6π-electrolization and subsequent aromatization. However, the yields of the reactions of bromobenzoporphyrin **4** with enynes were low due to severe polymerization reaction of enynes as well as a side reaction occurring to enynes in the presence of Pd(0).[63, 64] Zinc insertion of **5**, **6** and **7** followed by hydrolysis of the ester groups

This journal is © The Royal Society of Chemistry 20xx

Please do not adjust margins

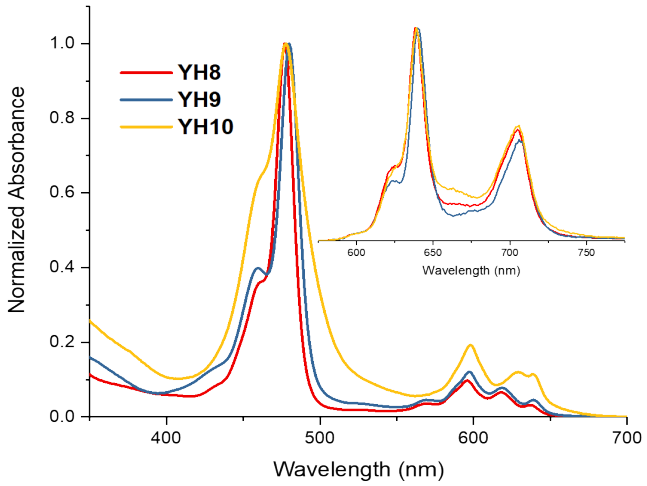

Figure 2 Normalized UV-Vis absorption spectra of **YH8** – **YH10** in THF. Inset: normalized fluorescence spectra of **YH8** – **YH10** in THF. The compounds were excited at the most intense visible band maxima

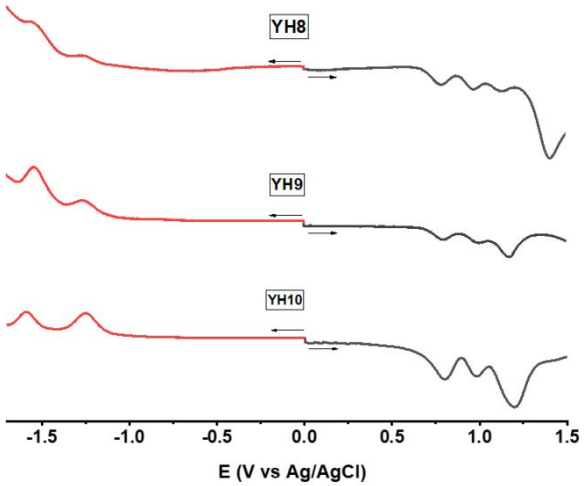

Figure 3 Differential pulse voltammograms of **YH8**-**YH10** (0.5 mM) in o-DCB with 0.1 M tetrabutylammonium perchlorate as the electrolyte, a platinum button working electrode, a platinum counter electrode, and an Ag/ AgCl reference electrode.

furnished the final push-pull *opp*-dibenzoporphyrins **YH8**, **YH9** and **YH10**, respectively.

2.2 Optical properties

Normalized UV-Vis absorption spectra of dibenzoporphyrins **YH8-YH10** are compiled in Fig. 2. Dibenzoporphyrin **YH9** bearing the diphenylamino-group displayed very similar absorption pattern with that of **YH7**,[56] with both showing an intense Soret band centered at 480 nm and an apparent shoulder at 460 nm for **YH9** and 458 nm for **YH7**. The Q bands of **YH9** and **YH7** are also similar. While **YH9** absorbed at 597, 618, 639 nm, the corresponding absorption bands of **YH7** were found at 598, 618, 641 nm. The minor differences between the absorption spectra of **YH9** and **YH7** reflect that the phenyl substituents of the amino group executed a minimal impact on the electronic properties of **YH9**, which is likely due to the non-planarity of the diarylamino group. Upon fusion of two phenyl groups, both the Soret bands of **YH8** and **YH10** shifted slightly hypsochromically and the shoulder of the Soret bands became less distinguishable. The Soret band of **YH10** was much more broadened relative to that of **YH9** and **YH8**. The Q bands of **YH8** shifted slightly hypsochromically and were narrowed relatively to those of **YH9**. In contrast, the Q bands of **YH10** were much more broadened and enhanced as compared to those of **YH8** and **YH9**. These data suggest the different influences of the carbazole (**YH8**) and phenothiazine (**YH10**) on the electronic properties of the dyes. **YH10** has much better spectral overlap with the solar spectrum arising from broadened and enhanced absorption which could contribute a better photovoltaic performance.

Steady-state fluorescence spectra of the three dibenzoporphyrins (**YH8**-**YH10**) exhibited similar emission patterns with two emission bands around 600 nm – 750 nm (Fig. 2, inset). The fluorescence spectra onset of **YH8-YH10** roughly reflect a similar trend in their UV-Vis absorption spectra. The optical data of these porphyrins are organized in Table 1.

The fluorescence lifetime of **YH8-YH10** were measured using time correlated single photon counting (TCSPC) technique. The fluorescence lifetimes of **YH8** and **YH9** were found to be 1.12 ns and 1.18 ns, respectively, both of which are slightly longer than that of **YH7** (1.06 ns). In contrast, the fluorescence lifetime of **YH10** was only 0.58 ns, suggesting even stronger push-pull effect in **YH10**.

The optical HOMO–LUMO energy gaps of **YH7**-**YH10** were calculated from UV-Vis and emission spectra. **YH8**-**YH10** displayed the same optical energy gaps of 1.94 eV, which is only slightly higher than that of **YH7** (1.93 eV).

2.3 Electrochemical characterization

The electrochemical properties of **YH8**-**YH10** were measured by cyclic (CV) and differential pulse voltammetric (DPV) techniques. All these three dibenzoporphyrins revealed two one-electron oxidations corresponding to porphyrin ring oxidations and a third multi-electron oxidation due to the peripheral push groups, and two one-electron reductions (Fig. 3, see Fig. S2 for CV curves). CV studies suggested these electrode processes to be quasi- to-irreversible, hence, DPV data was used to report the redox potential values. The two oxidations occurred at 0.78 V and 0.99 V vs. Ag/AgCl for **YH9**, which are close to those of **YH7** (0.78 V and 0.96 V). The carbazole bearing **YH8** was relatively easier to oxidize than **YH9** with the first oxidation found at 0.77 V and second oxidation at 0.97 V. In contrast, **YH10** revealed relatively higher oxidation potential with the first one at 0.79 V and second one at 0.98 V. While the reduction potential of **YH8** (-1.22), **YH9** (-1.25 V) and **YH10** (-1.24 V) shifted to more negative potentials as compared with **YH7** (-0.96). These electrochemical data once again reflect the impact of the different 3° arylamine donor groups on the electronic properties of the porphyrins. The electrochemical HOMO–LUMO energy gap followed the order of **YH7** (2.06 V) > **YH10** (2.03 V) ~ **YH9** (2.03 V) > **YH8** (1.99 V). Although electrochemical HOMO–LUMO gap is slightly higher from their optical HOMO–LUMO gap, it is notable that the electrochemical

This journal is © The Royal Society of Chemistry 20xx

Please do not adjust margins

energy gap of **YH7**, **YH9** and **YH10** are very close, roughly following a similar trend observed for the optical energy gap.

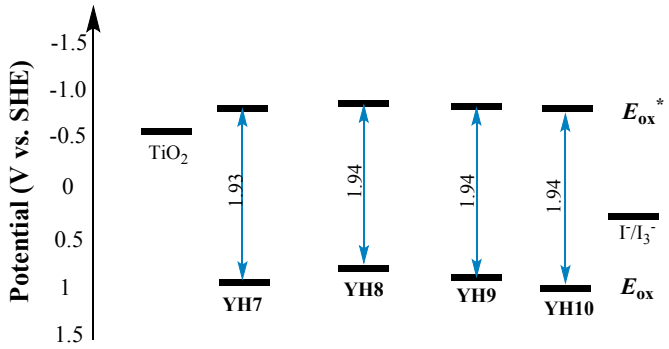

Figure 4 Energy level diagram of HOMO and LUMO of **YH7**, **YH8**, **YH9** and **YH10.**

The relevant optical and electrochemical data are compiled in Table 1.

The driving force for dye regeneration (ΔG_{reg}) of oxidized dyes was estimated using the experimental first oxidation potentials of **YH8**-**YH10** and the potential of the redox mediator I^-/I_3^- (Fig. 4). All investigated porphyrins possess first oxidation potentials > 0.5 V, more positive than the potential of the redox mediator I^-/I_3^- (0.42 V vs SHE) (Table 1), which suggest thermodynamically feasible regeneration of oxidized dyes from electron mediator.

The driving force for electron injection (ΔG_{inj}) from the excited dye to the conduction band of the TiO_2 was also determined (Fig. 4). The excited state oxidation potentials (E_{ox}*) of **YH7**-**YH10** were calculated to be -0.94 V, -0.97 V, -0.96 V and -0.94 V, respectively. The LUMO energy levels are sufficiently high to ensure efficient electron injection from the photo-excited porphyrin dyes to the conduction band of the TiO_2 (ΔG_{inj} = -0.44 to -0.47 eV).

2.4 DFT calculations

DFT calculations (*Gaussian 09* DFT B3LYP/6-31G(d,p) in gas phase) were carried out for **YH8**-**YH10** in order to gain better understanding of their electronic properties. The calculated geometries (Fig. 5, top) and the HOMOs and LUMOs (Fig. 5, bottom) of these molecules are shown in Figure 5. Dibenzoporphyrin **YH8**-**YH10** adopt slightly domed conformation. It is notable that the phenylethynyl groups in **YH8**-**YH10** lie in the same plane with the porphyrin core, which is expected to facilitate intramolecular electronic communications.

The LUMOs of these porphyrins mainly involve the porphyrin core and the acceptor groups including the phenylethynyl component bearing the anchoring groups. The donor groups are not included in the LUMO and LUMO+1. The HOMO of **YH9** is mainly located at the donor group. It is interesting to note that the HOMO and HOMO-1 of **YH10** reside on one of the phenothiazine group. The characteristics of the

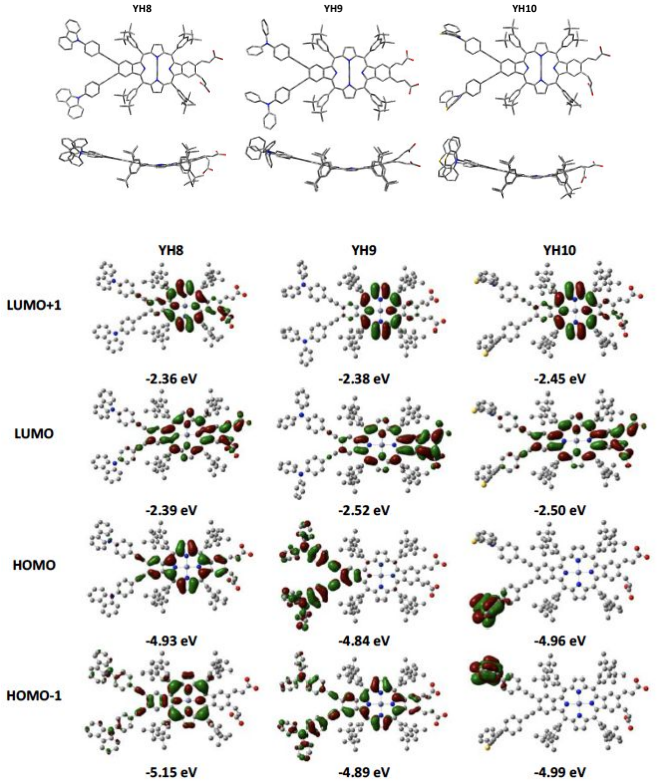

Figure 5 Geometry-optimized molecule structures of **YH8**-**YH10** (Top) and Isodensity surface of LUMO+1, LUMO, HOMO, HOMO-1 for **YH8**-**YH10** calculated by *Gaussian09* DFT B3LYP/6-31G(d,p). Hydrogen atoms were omitted for clarity

HOMOs and LUMOs of **YH9** and **YH10** suggest significant orbital segregation. Such orbital segregation is expected to facilitate electron injection from the photoexcited dye to the TiO_2 conduction band.[13, 65] It is notable that the orbital arrangement of **YH9** is very similar to that of **YH7**. In contrast, **YH8** displays a completely different feature. The HOMO of **YH8** is mainly located at the porphyrin core with some contributions on the two fused benzene rings. The HOMO-1 of **YH8** is also located at the porphyrin core, however, with inclusion of only one fused benzene ring. The donor group are not involved in both the HOMO and HOMO-1 of **YH8**. The energy levels of orbital also displayed a different scenario. While the HOMO and HOMO-1 for **YH9** and **YH10** remain essentially degenerated, the degeneracy of the HOMO and HOMO-1 for **YH8** is broken. On the other hand, while the LUMO and LUMO+1 of **YH8** is degenerated, those of **YH9** and **YH10** are more split. The calculated data on the molecular orbitals explain the significant difference on the electronic and electrochemical properties observed for **YH8**, **YH9** and **YH10**.

The order of the calculated HOMO-LUMO energy gap is **YH8** (2.53 eV) > **YH10** (2.46 eV) > **YH9** (2.32 eV) ~ **YH7** (2.38 eV). This order does not agree with those of the optical energy gap and electrochemical energy gap. The discrepancy could be explained with solvent effects as the optical and electrochemical measurements were performed in different solvents.

DFT calculations (*Gaussian 09* DFT B3LYP/6-31G(d,p)) in acetonitrile were carried out for **YH8**-**YH10** to further understand how inclusion of solvent would affect the DFT

This journal is © The Royal Society of Chemistry 20xx

Please do not adjust margins

Table 1 Absorption, fluorescence, ground and excited state oxidation potentials of the investigated porphyrins, and the free-energy change for charge injection and recombination involving the porphyrins and TiO_2

Dye	λ_{max}^{abs}[a] [nm] (ε, 10^5 M^{-1} cm^{-1})	λ_{max}^{em}[a] [nm]	$E_{0\text{-}0}$ [b] [eV]	E_{ox} [c] [V]	E_{ox}^* [d] [V]	ΔG_{inj} [e] [eV]	ΔG_{reg} [f] [eV]
YH7	480 (2.11)	644, 709	1.93	0.99	-0.94	-0.44	-0.57
YH8	477 (4.41)	638, 705	1.94	0.97	-0.97	-0.47	-0.55
YH9	480 (2.95)	640, 706	1.94	0.98	-0.96	-0.46	-0.56
YH10	478 (2.12)	639, 706	1.94	1.00	-0.94	-0.44	-0.58

[a] Wavelength of the absorption and emission maxima in THF; The extinction coefficients (ε, 10^5 M^{-1} cm^{-1}) are shown in parentheses. [b] $E_{0\text{-}0}$ was determined from the intersection of normalized absorption and emission spectra. [c] The oxidation potentials of dyes were measured in *o*-DCB with 0.1 M $(TBA)ClO_4$; Potentials measured vs. the Ag/AgCl (Ag/Ag^+) couple were converted to potential vs. SHE. [d] Excited-state oxidation potentials (E_{ox}^*) was approximated from E_{ox} and $E_{0\text{-}0}$. [e] Driving force for electron injection (ΔG_{inj}) calculated from the energy difference between the dye excited state oxidation potential (E_{ox}^*) and conduction band of TiO_2 (-0.5 V vs. SHE). [f] Driving force for regeneration (ΔG_{reg}) calculated from the energy difference between the porphyrin oxidation potential (E_{ox}) and the iodine redox (I^-/I_3^-) couple (+0.42 V vs. SHE).

calculations. The calculated geometries and frontier orbitals of **YH8**-**YH10** are compiled in Fig. S4 in the Supporting Information. It is not surprising that the orbital distributions of the HOMOs and LUMOs of **YH8**-**YH10** changed in acetonitrile media. While the HOMO and LUMO of **YH10** displayed even enhanced segregation, the segregation of the HOMO and LUMO of **YH9** became much less significant. On the other hand, the HOMO and LUMO of **YH8** remained similar to those of the DFT calculation in gas phase. These data provide some insights into solvent effects on understanding solar cell performance.

2.5 Photovoltaic performance

DSSCs sensitized by **YH8**-**YH10** were assembled and photocurrent-voltage (*J*-*V*) curves and IPCE action spectra were performed to evaluate the photovoltaic performance of the DSSCs. The *J*-*V* curves and IPCE spectra were measured under simulated AM 1.5 one sun (100 mW cm^{-2}) illumination on cells with a 0.16 cm^2 active area. The sandwich type two electrode cells were constructed of working electrode, dye-coated TiO_2 film, Pt-ized FTO as counter electrode, and a I^-/I_3^- as redox mediator in presence of $CHCl_3$/t-BuOH (v/v, 1/2) solvent mixture. The steady photocurrent production was confirmed by preforming on-off switching experiments. The light to power conversion efficiency (η) was determined based on equation (1), where J_{SC} is short-circuit current density, V_{OC} is open circuit voltage, and FF is fill factor.

$$\eta = J^{SC} \times V^{OC} \times FF \qquad (1)$$

The calculated η values for the best of three cells are organized in Table 2.

2.5.1 Dye adsorption time and dye aggregation effect

Dye soaking time for dye adsorption on TiO_2 surface was investigated to optimize solar cell performance using **YH10** as the standard sensitizer (Table S5 in ESI). A range of times were tested including 3h, 6h, 9h, 12h and 15h. It turned out that 3h of dye soaking time gave the optimal photovoltaic performance. The PCE value of **YH10** decreased significantly with increased soaking time, which suggests severe dye aggregation at higher dye concentration on the photoanode, leading to lower J_{SC} and V_{OC} values.

Dye aggregation is known to ensue self-quenching of the excited state, thus block the pathways to carrier photogeneration resulting in low photovoltaic performance. To optimize the dye adsorption on TiO_2 surface, we investigated the dye concentration and the solvent ratio ($CHCl_3$/t-BuOH) using **YH10** (see Tables S2 and S3 in ESI). A dye concentration of 0.2 mM in 2/1 (v/v) of $CHCl_3$/t-BuOH gave the best power conversion efficiency. Co-adsorption of chenodeoxycholic acid (CDCA) with the dye onto the TiO_2 surface is an effective strategy to reduce dye aggregation. The effect of CDCA was then investigated through sensitizing **YH10** with different concentrations of CDCA (0 mM– 1.0 mM CDCA) (see Table S4 in ESI). The best PCE value was achieved when 0.2 mM CDCA was used as a co-absorbent with **YH10**.

2.5.2 Power conversion efficiency

The power conversion efficiencies were measured for solar cells based on **YH8**-**YH10** under optimized conditions. The photovoltaic performances of these solar cells are organized in in Fig. 6 and Table 2. The power conversion efficiency (PCE, η) of the **YH9**-sensitized solar cell is 6.9%, which was much higher than that of its aliphatic counterpart **YH7** (5.7%) bearing dimethylamino group as the donor group. The increased PCE can be attributed to the improved stability of **YH9** in the presence of the I_2/I_3^- electrolyte. In sharp contrast to **YH7**-based solar cell, for which significant decomposition was observed causing the dark green-coloured surface of the **YH7**-sensitized device to turn to a pale colour upon irradiation, **YH9**-based solar cell was stable with no observable colour change upon irradiation. The **YH8-** and **YH10**-based solar cells displayed similar stability. The much-enhanced stability of the **YH8**-**YH10** based solar cells suggests that the strategy of utilizing arylamines to replace aliphatic amines as the donor group of the dyes is effective.

YH10-sensitized solar cells achieved even higher PCE (η = 7.5%) than the **YH9** cell, making it comparable with the best Ruthenium dye N719 (η = 7.7%). The V_{oc} values of **YH9** and **YH10**

Table 2 Photovoltaic performance of DSSCs based on **YH8**, **YH9** and **YH10**

Dye[a]	J_{SC} (mA/cm^2)	V_{OC} (V)	FF	η (%)
YH8	12.51	0.6	0.72	5.3[c]
YH9	16.16	0.63	0.68	6.9[c]
YH10	17.16	0.63	0.70	7.5[c]
YH7[b]	15.12	0.57	0.66	5.7[c]

The photovoltaic measurements were conducted under AM 1.5G illumination (power 100 mW cm^{-2}) in the presence of a mask and with a cell active area of 0.16 cm^2 and a TiO_2 thickness of 25 µm. As a reference, efficiency of **N719**-sensitized solar cells was determined: J_{SC} = 16.5 mA cm^{-2}, V_{OC} = 0.67 V, FF = 0.63, and η = 7.7%.
[a] The TiO_2 film was soaked in 0.3 mM dye solution in ($CHCl_3$/t-BuOH) (v/v = 1/2) containing 0.2 mM CDCA for 3 h. [b] The TiO_2 film was soaked in 0.2 mM dye solution in MeOH/$CHCl_3$ (v/v = 1/1) without CDCA for 3 h. [c] Best device PCE.

cells are the same at 0.63 V, indicating similar kinetic processes for electron injection and charge collection (TiO_2). The J_{SC} value of **YH10** cell is higher than that of **YH9** cell (16.16 mA/cm^2), reaching 17.16 mA/cm^2. The higher J_{SC} value of **YH10** cell suggests the higher light harvesting ability of **YH10** as reflected by the much broader UV-Vis absorption spectrum. A silent factor that also contributes to the much higher PCE of **YH10** cell is the HOMO orbital distribution of **YH10** (Figure 5), which is much further away from the TiO_2 surface as compared with those of **YH8** and **YH9**. The longer distance from TiO_2 surface is expected to retard charge recombination and thus enhance PCE.[66]

When carbazole groups serve as the donor group, the **YH8**-sensitized solar cell gave a surprisingly low PCE of 5.3%, even lower than the solar cell sensitized by **YH6** (6.7%), which does not bear electron-donating groups as donor groups.[56] The J_{SC} value of **YH8** cell (12.51 mA/cm^2) is much lower than those of **YH9** (16.16 mA/cm^2) and **YH10** (17.16 mA/cm^2) solar cells. The V_{oc} value (0.60 V) of **YH8** cell is also lower than those of the **YH9** (0.63 V) and **YH10** (0.63 V) cells. As shown in the UV-vis spectra (Fig. 2), **YH8** displayed much narrower Soret and Q bands as compared with **YH10**. However, the absorption bands of **YH8** are only slightly blue-shifted and narrower than those of **YH9**. On the other hand, the HOMOs and LUMOs of **YH9** and **YH10** showed orbital segregation with the LUMO lying heavily on the electron-withdrawing (anchoring) groups and the HOMO centred at the electron-donating groups. Such orbital segregation is expected to facilitate electron injection and charge separation, which is a much-desired feature for DSSC. In contrast, the HOMO and LUMO of **YH8** did not show any orbital segregation. This feature along with the earlier discussed free-energy change values (Table 1) are likely the reason for the low PCE of the **YH8** cell.

The current and potential switching plots are shown in Fig. 6c and Fig. 6d. The reproducibility of the results for **YH8**-**YH10** suggests the robustness of the solar cells.

2.5.3 IPCE values

The incident photon-to-current efficiency (IPCE%) spectra were measured for selected dye-sensitized devices (Fig. 6b). The IPCE% (λ) values were calculated from equation (2), where LHE is the light harvesting efficiency, Φ_{inj} is the quantum yield of

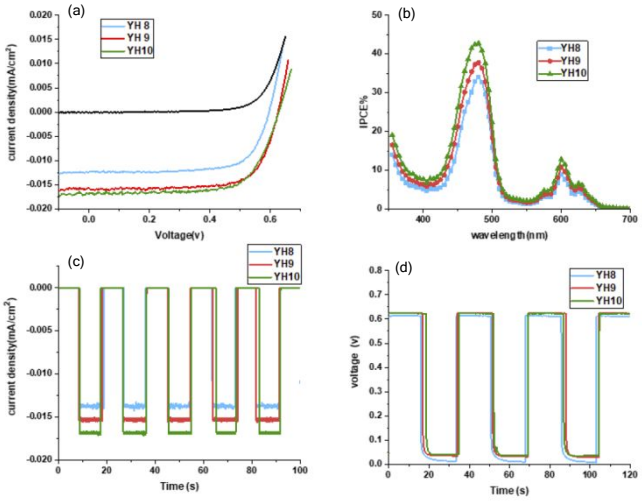

Figure 6 (a) J-V plots, (b) IPCE curves, (c) current switching and (d) potential switching of DSSCs developed in the present study

electron injection from the excited sensitizer into TiO_2, and η_{col} is the electron collection efficiency.

$$IPCE\ (\lambda) = LHE \times \Phi_{inj} \times \eta_{col} \qquad (2)$$

The IPCE% spectra of **YH8**-**YH10** display similar trend with higher IPCE values at the Soret band region (up to 45%) and lower IPCE values at the Q band region (up to 15%). **YH10** solar

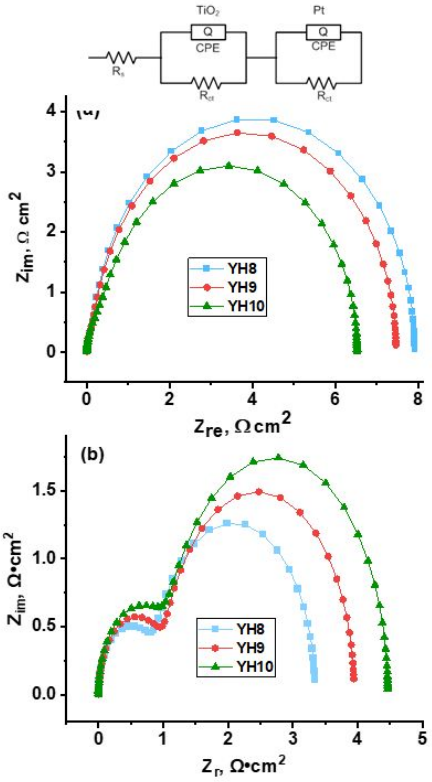

Figure 7 Nyquist plots for (a) FTO/TiO_2/(**YH8**-**YH10**) measured at respective V_{OC} under (a) dark and (b) AM 1.5 filtered light illumination conditions

cells exhibited higher IPCE values than **YH8** and **YH9** solar cells at both the Soret band region and Q-band region. The order of

This journal is © The Royal Society of Chemistry 20xx

Please do not adjust margins

the overall IPCE value is **YH10** > **YH9** and > **YH8**, which reflects exactly the trend observed for J_{SC}.

2.5.4 Electrochemical Impedance Spectroscopy (EIS) studies

The interfacial charge transfer resistance in solar cells were estimated with EIS experiments under dark and light conditions (Fig. 7).

The Nyquist plots of **YH8-YH10** show two semicircles with two different radii, whereas the larger semicircle in low frequency represent the electron transport at TiO_2/dye/redox mediator interface at the working electrode. The smaller semicircle in the high frequency relates to the charge transfer at the counter electrode/electrolyte interface. By using the equivalent circuit shown at the top of Fig. 7, the impedance curves of dyes were analyzed and the recombination resistance values (R_{ct}) were calculated. R_{ct} values for **YH8** (2.47 Ω cm^2) is lower than **YH9** and **YH10** (3.20 and 3.40 Ω cm^2, respectively) under light conditions (see Table 3) which generally agrees with high V_{oc} values recorded for the latter two compounds.

Table 3. Recombination Resistance for working electrodes of **YH8-YH10** estimated from EIS method.

Dye	Condition	R_{rec}, Ω•cm^2
YH8	Dark	7.76
	Light	2.47
YH9	Dark	7.28
	Light	3.20
YH10	Dark	6.14
	Light	3.40

2.5.5 Photodegradation investigation

In the previous work,[56] we observed that **YH7** (see Fig. 1 for structure of **YH7**) solar cell became discoloured 5-10 mins after the solar cell was assembled. Discolouration of **YH6** solar cell was not observed. Solar cell stability studies revealed that PCE of **YH6** cell increased in 3 h and only slightly decreased after 20 h. In contrast, PCE of **YH7** cell continually decreased within the 20 h window. In order to understand the causes of the degradation, we conducted stability studies for **YH6** and **YH7** in solution and on TiO_2 surface (see Fig. S5 and S6 in ESI) using UV-Vis spectroscopy. Our studies showed that **YH6** and **YH7** display similar stability in solution and on TiO_2 surface. However, when I_2/I_3- was present, **YH7** bearing amine groups decomposed much faster than **YH6** that does not carry amine groups in solution (see Fig. S7 in ESI), which correlates well with the phenomenon observed for the corresponding solar cells. It has been reported that the presence of triethanolamine (TEA) facilitates the photobleaching of porphyrins.[57] It is likely that the tertiary amine groups on **YH7** caused the severe degradation in the presence of I_2/I_3^- electrolyte.

Since **YH7** demonstrated much stronger push-pull effect than **YH6**, which was a much-desired feature for dyes in DSSC, we decided to investigate the possibility to replace the amine group in **YH7** with arylamines as the donating groups. **YH8**, **YH9** and **YH10** bearing arylamines, i.e., carbazole (**YH8**), diphenylamine (**YH9**) and phenothiazine (**YH10**), displayed similar stabilities with **YH7** in solution in the absence of I_2/I_3^-. When I_2/I_3^- was present, **YH8**-**YH10** also showed similar decomposition profiles with that of **YH7** (see Fig. S8 in ESI). In sharp contrast with the **YH7** solar cell, **YH8**-**YH10** based solar cells showed similar stability with **YH6** cell during the measurement time period. These data suggest that the bulky tertiary arylamine of **YH8**-**YH10** could stabilize the solar cells likely through shielding the amine group from interacting with the electrolyte on TiO_2 surface. However, in solution, such shielding does not exist, as a result, all these amine carrying dyes share similar decomposition profiles in solution.

3. Conclusions

In summary, a series of *β*-functionalized push-pull *opp*-dibenzoporphyrins bearing different push groups (**YH8–YH10**) has been introduced as sensitizers for dye-sensitized solar cells. These compounds were designed to solve the solar cell instability issue reported earlier. Replacing alkylamines with arylamines as the donor groups proved to be an effective strategy to alleviate the problem of illumination-induced dye degradation. The presence of two anchoring groups, a unique structural advantage of these benzoporphyrin dyes as compared with the majority of other organic dyes carrying only one anchoring group, further enhances the solar cell stability. Remarkably high PCEs close to the best ruthenium **N719** dye (η = 7.7%) have been achieved with **YH9** (η = 6.9%) and **YH10** (η = 7.5%). The high PCE of **YH10** solar cell is mainly attributed to its exceptional light harvesting ability and favourable cell kinetics. In addition, the orbital distribution in the HOMO of **YH10** is further away from TiO_2 surface relative to those of **YH8** and **YH9**, which is expected to slow down the charge recombination and contribute to its higher PCE. The results in this work suggest the great potential of *β*-functionalized push-pull *opp*-dibenzoporphyrins, representing a new generation of sensitizers for DSSC. We anticipate new breakthroughs achieved with *β*-functionalized push-pull *opp*-dibenzoporphyrins in DSSC.

Significant push groups effects were observed for these porphyrins. Different amino groups including carbazole (**YH8**), diphenylamine (**YH9**) and phenothiazine **YH10** were incorporated into the dye molecules as the donor group. Push-pull dibenzoporphyrins bearing diphenylamine (**YH9**) and phenothiazine (**YH10**) demonstrated strong push-pull effects, displaying significant orbital segregation with the LUMO heavily located at the anchoring groups (acrylic acid groups) and HOMO centred at the donor groups. All these push-pull porphyrins (**YH8**-**YH10**) showed red-shifted and broadened absorption bands as compared with **YH6** bearing no donor groups. The band broadening was particularly remarkable for phenothiazine carrying **YH10**. The fluorescence lifetime of **YH10** (0.58 ns) was also much shorter than those of **YH8** (1.12 ns) and **YH9** (1.18 ns). In sharp contrast, the inclusion of carbazole group as the donor group (**YH8**) rendered an opposite effect. The absorption bands of **YH8** were blue shifted, and much narrower than those of **YH10**. The significant orbital segregation observed for **YH7**, **YH9** and **YH10** did not appear on the HOMO and LUMO of **YH8**. The HOMO and LUMO energy levels of **YH8** were largely elevated as

Please do not adjust margins

compared with those of **YH7**, **YH9** and **YH10**. As a result, The **YH8** solar cell gave the lowest PCE of 5.3%. The notable differences in the electronic and optical properties of these dibenzoporphyrins indicate their exceptional structural modifiability. Further Investigation into structural-property-efficiency relationships of this class of benzoporphyrins is currently underway in our laboratories.

Conflicts of interest

There are no conflicts to declare.

Acknowledgements

This work was supported by the U.S. Department of Energy, Office of Science, Basic Energy Sciences under Award (DE-SC0016766). Our gratitude goes out to Dr. Guido Verbeck and the Laboratory for Imaging Mass Spectrometry at the University of North Texas for MALDI-Orbitrap Mass Spectrometry data.

Notes and references

1 A. Hagfeldt, G. Boschloo, L. Sun, L. Kloo and H. Pettersson, *Chem. Rev.*, 2010, **110**, 6595-6663.
2 B. O'Regan and M. Grätzel, *Nature,* 1991, **353**, 737-740.
3 L. M. Gonçalves, V. de Zea Bermudez, H. A. Ribeiro and A. M. Mendes, *Energy. Environ. Sci.*, 2008, **1**, 655.
4 A. Kay and M. Graẗzel, *J. Phys. Chem.*, 1993, **97**, 6272-6277.
5 A. Reynal and E. Palomares, *Eur. J. Inorg. Chem.*, 2011, **2011**, 4509-4526.
6 L. Zayat, O. Filevich, L. M. Baraldo and R. Etchenique, *Philosophical transactions. Series A, Mathematical, physical, and engineering sciences*, 2013, **371**, 20120330.
7 G. Di Carlo, A. O. Biroli, F. Tessore, S. Caramori and M. Pizzotti, *Coord. Chem. Rev.*, 2018, **358**, 153-177.
8 T. N. Murakami and N. Koumura, *Adv. Energy Mater.*, 2018, **9**. 1802967.
9 J. M. Cole, G. Pepe, O. K. Al Bahri and C. B. Cooper, *Chem. Rev.*, 2019, **119**, 7279-7327.
10 I. Obraztsov, W. Kutner and F. D'Souza, *Solar RRL*, 2017, **1**, 1600002.
11 H. Song, Q. Liu and Y. Xie, *Chem. Commun.*, 2018, **54**, 1811-1824.
12 M. Urbani, G. de la Torre, M. K. Nazeeruddin and T. Torres, *Chem. Soc. Rev.*, 2019, **48**, 2738-2766.
13 C.-W. Lee, H.-P. Lu, C.-M. Lan, Y.-L. Huang, Y.-R. Liang, W.-N. Yen, Y.-C. Liu, Y.-S. Lin, E. W.-G. Diau and C.-Y. Yeh, *Chem. Eur. J.*, 2009, **15** 1403 – 1412.
14 S. Mathew, A. Yella, P. Gao, R. Humphry-Baker, B. F. Curchod, N. Ashari-Astani, I. Tavernelli, U. Rothlisberger, M. K. Nazeeruddin and M. Gratzel, *Nat. Chem.*, 2014, **6**, 242-247.
15 J. P. Hill, *Angew Chem Int Ed Engl*, 2016, **55**, 2976-2978.
16 C.-L. Wang, J.-Y. Hu, C.-H. Wu, H.-H. Kuo, Y.-C. Chang, Z.-J. Lan, H.-P. Wu, E. Wei-Guang Diau and C.-Y. Lin, *Energy Environ. Sci.*, 2014, **7**, 1392.
17 A. Yella, H.-W. Lee, H. N. Tsao, C. Yi, A. K. Chandiran, M. K. Nazeeruddin, E. W.-G. Diau, C.-Y. Yeh, S. M. Zakeeruddin and M. Grätzel, *Science*, 2011, **334**, 629-634.
18 A. Yella, C. L. Mai, S. M. Zakeeruddin, S. N. Chang, C. H. Hsieh, C. Y. Yeh and M. Gratzel, *Angew. Chem. Int. Ed. Engl.*, 2014, **53**, 2973-2977.
19 T. Bessho, S. M. Zakeeruddin, C. Y. Yeh, E. W. Diau and M. Gratzel, *Angew. Chem. Int. Ed. Engl.*, 2010, **49**, 6646-6649.
20 Y. Kurumisawa, T. Higashino, S. Nimura, Y. Tsuji, H. Iiyama and H. Imahori, *J. Am. Chem. Soc.*, 2019, **141**, 9910-9919.
21 J. M. Ji, H. Zhou, Y. K. Eom, C. H. Kim and H. K. Kim, *Adv. Energy Mater.*, 2020, **10**, 2000124.
22 K. Zeng, Y. Chen, W. H. Zhu, H. Tian and Y. Xie, *J. Am. Chem. So.c*, 2020, **142**, 5154-5161.
23 J. Zhang, C.-J. Chen and H.-C. Zhu, *Appl. Surf. Sci.*, 2020, **513**, 145844.
24 J. Zou, Q. Yan, C. Li, Y. Lu, Z. Tong and Y. Xie, *ACS Appl. Mater. Interfaces*, 2020, **12**, 57017-57024.
25 Y. Tang, Y. Wang, Q. Yan, K. Zeng, W. Tang, S. Zhao, C. Kong and Y. Xie, *Dyes Pigm.*, 2021, **187**.
26 Y. Wu, W. H. Zhu, S. M. Zakeeruddin and M. Gratzel, *ACS Appl. Mater. Interfaces*, 2015, **7**, 9307-9318.
27 T. Higashino and H. Imahori, *Dalton Trans.*, 2015, **44**, 448-463.
28 B. J. Brennan, M. J. Llansola Portoles, P. A. Liddell, T. A. Moore, A. L. Moore and D. Gust, *Phys. Chem. Chem. Phys.*, 2013, **15**, 16605-16614.
29 N. Kobayashi, *Chem. Phys. Lett.* , 1993, **205**, 51-54.
30 T. D. Lash, *J. Porphyrins Phthalocyanines*, 2001, **5**, 267-288.
31 S. Hayashi, M. Tanaka, H. Hayashi, S. Eu, T. Umeyama, Y. Matano, Y. Araki and H. Imahori, *J. Phys. Chem. C*, 2008, **112**, 15576-15585.
32 A. V. Cheprakov and M. A. Filatov, *J. Porphyrins Phthalocyanines*, 2009, **13**, 291-303.
33 N. Ono, H. Yamada and T. Okujima, *Synthesis of Porphyrins Fused with Aromatic Rings,* World Scientific Publ., Singapore, 2010.
34 L. J. K. Boerner, S. Mazumder, M. Pink, J. M. Zaleski and M.-H. Baik, *Chem. Eur. J.*, 2011, **17**, 14539 – 14551.
35 A. V. Cheprakov, *The Synthesis of pi-Extended Porphyrins*, World Scientific Publ., Singapore, 2011.
36 C.-L. Wang, Y.-C. Chang, C.-M. Lan, C.-F. Lo, E. Wei-Guang Diau and C.-Y. Lin, *Energy Environ. Sci.*, 2011, **4**, 1788.
37 J. M. Ball, N. K. S. Davis, J. D. Wilkinson, J. Kirkpatrick, J. Teuscher, R. Gunning, H. L. Anderson and H. J. Snaith, *RSC Adv.*, 2012, **2**, 6846-6853.
38 C. M. Carvalho, T. J. Brocksom and K. T. de Oliveira, *Chem. Soc. Rev.*, 2013, **42**, 3302-3317.
39 V. V. Roznyatovskiy, C. H. Lee and J. L. Sessler, *Chem. Soc. Rev.*, 2013, **42**, 1921-1933.
40 A. Chaudhary, A. Srinivasan and T. K. Chandrashekar,, *Handbook of Porphyrin Science,* World Scientific Publ., Singapore, 2014.
41 M. Ishida, D. Hwang, Y. B. Koo, J. Sung, D. Y. Kim, J. L. Sessler and D. Kim, *Chem. Commun.*, 2013, **49**, 9164-9166.
42 M. Ishida, D. Hwang, Z. Zhang, Y. J. Choi, J. Oh, V. M. Lynch, D. Y. Kim, J. L. Sessler and D. Kim, *ChemSusChem*, 2015, **8**, 2967-2977.
43 M. Ishida, S. W. Park, D. Hwang, Y. B. Koo, J. L. Sessler, D. Y. Kim and D. Kim, *J. Phys. Chem. C*, 2011, **115**, 19343-19354.
44 H. Hayashi, A. S. Touchy, Y. Kinjo, K. Kurotobi, Y. Toude, S. Ito, H. Saarenpaa, N. V. Tkachenko, H. Lemmetyinen and H. Imahori, *ChemSusChem*, 2013, **6**, 508-517.
45 H. Imahori, H. Iijima, H. Hayashi, Y. Toude, T. Umeyama, Y. Matano and S. Ito, *ChemSusChem*, 2011, **4**, 797-805.
46 A. Kira, Y. Matsubara, H. Iijima, T. Umeyama, Y. Matano, S. Ito, M. Niemi, N. V. Tkachenko, H. Lemmetyinen and H. Imahori, *J. Phys. Chem. C*, 2010, **114**, 11293-11304.
47 R. Deshpande, B. Wang, L. Dai, L. Jiang, C. S. Hartley, S. Zou, H. Wang and L. Kerr, *Chem. Asian J.*, 2012, **7**, 2662-2669.
48 F. Lodermeyer, R. D. Costa, J. Malig, N. Jux and D. M. Guldi, *Chem. Eur. J*, 2016, **22**, 7851-7855.
49 G. Zanotti, N. Angelini, G. Mattioli, A. M. Paoletti, G. Pennesi, G. Rossi, D. Caschera, L. d. Marcoc and G. Giglide, *RSC Adv.*, 2016, **6**, 5123 - 5133.
50 M. Ishida, S. W. Park, D. Hwang, Y. B. Koo, J. L. Sessler, D. Y. Kim and D. Kim, *J. Phys. Chem. C*, 2011, **115**, 19343–19354.

This journal is © The Royal Society of Chemistry 20xx

Please do not adjust margins

51 F. Lu, Y. Feng, X. Wang, Y. Zhao, G. Yang, J. Zhang, B. Zhang and Z. Zhao, *Dyes Pigm.*, 2017, **139**, 255-263.
52 R. Deshpande, L. Jiang, G. Schmidt, J. Rakovan, X. Wang, K. Wheeler and H. Wang, *Org. Lett.*, 2009, **11**, 4251-4253.
53 L. Jiang, J. T. Engle, L. Sirk, C. S. Hartley, C. J. Ziegler and H. Wang, *Org. Lett.*, 2011, **13**, 3020-3023.
54 R. G. Jinadasa, Y. Fang, S. Kumar, A. J. Osinski, X. Jiang, C. J. Ziegler, K. M. Kadish and H. Wang, *J. Org. Chem.*, 2015, **80**, 12076-12087.
55 S. Kumar, X. Jiang, W. Shan, R. G. W. Jinadasa, K. M. Kadish and H. Wang, *Chem. Commun.*, 2018, **54**, 5303-5306.
56 Y. Hu, W. A. Webre, M. B. Thomas, A. Moss, S. N. Hancock, J. Schaffner, F. D'Souza and H. Wang, J. Mater. Chem. A, 2019, 7, 10712-10722.
57 G. R. Soja and D. F. Watson, Langmuir, 2009, 25, 5398-5403.
58 T.-H. Huang, W.-T. Whang, J. Y. Shen, J. T. Lin and H. Zheng, J. Mater. Chem., 2005, 15.
59 E. M. Barea, V. Gónzalez-Pedro, T. Ripollés-Sanchis, H.-P. Wu, L.-L. Li, C.-Y. Yeh, E. W.-G. Diau and J. Bisquert, J. Phys. Chem. C, 2011, 115, 10898-10902.
60 C.-P. Hsieh, H.-P. Lu, C.-L. Chiu, C.-W. Lee, S.-H. Chuang, C.-L. Mai, W.-N. Yen, S.-J. Hsu, E. W.-G. Diau and C.-Y. Yeh, J. Mater. Chem., 2010, 20, 1127-1134.
61 R. G. Jinadasa, B. Li, B. Schmitz, S. Kumar, Y. Hu, L. Kerr and H. Wang, ChemSusChem, 2016, 9, 2239-2249.
62 Y. Hu, S. Yellappa, M. B. Thomas, R. G. W. Jinadasa, A. Matus, M. Shulman, F. D'Souza and H. Wang, Chem. Asian J., 2017, 12, 2749-2762.
63 V. Gevorgyan, N. Tsuboya and Y. Yamamoto, J. Org. Chem., 2011, 66, 2743-2746.
64 F. Punner and G. Hilt, Chem. Commun., 2012, 48, 3617-3619.
65 C.-P. Hsieh, H.-P. Lu, C.-L. Chiu, C.-W. Lee, S.-H. Chuang, C.-L. Mai, W.-N. Yen, S.-J. Hsu, E. W.-G. Diau and C.-Y. Yeh, J. Mater. Chem., 2010, 20, 1127-1134.
66 M. Urbani, M. Grätzel, M. K. Nazeeruddin and T. Torres , Chem. Rev., 2014, **114**, 12330-12396.

This journal is © The Royal Society of Chemistry 20xx

Please do not adjust margins